Korean J. Chem. Eng., 35(9), 1941-1947 (2018)
DOI: 10.1007/s11814-018-0088-7

pISSN: 0256-1115
eISSN: 1975-7220

Preparation of PEDOT-ordered mesoporous carbon hybrid material using vapor phase polymerization

Pauline May Losaria*, Young Soo Ko, and Jin-Heong Yim*,†**

*Division of Advanced Materials Engineering, Kongju National University,
1223-24 Cheoandaero, Cheonan, Chungnam 31080, Korea
**Department of Chemical Engineering, Kongju National University,
1223-24 Cheoandaero, Cheonan, Chungnam 31080, Korea
(*Received 8 March 2018 • accepted 27 May 2018*)

Abstract−A hybrid composite was prepared by the formation of poly (3,4-ethylenedioxythiophene) (PEDOT) layer on two types of ordered mesoporous carbon (OMC) by vapor phase polymerization. The morphology, chemical composition, pore structure, and electrical properties of the normal type ordered mesoporous carbon (NTOMC) and rod type ordered mesoporous carbon (RTOMC) composites were compared and analyzed. The surface morphology of the PEDOT-OMC composite did not change, due to the uniform coating of PEDOT layer on the OMC. The content of PEDOT in the composite and the thickness of the coating layer both increased with the amount of the oxidizing agent, Iron (III) *p*-toluenesulfonate (FTS) used in VPP. Pore size, porosity, and surface area of PEDOT-OMC composite decreased with coating of PEDOT layer on the outer surface of the OMC, and the mesopore inner wall. Electrical resistance decreased with an increase in the thickness of the PEDOT layer coated on the OMC. The PEDOT-RTOMC composite had lower electrical resistivity than the PEDOT-NTOMC composite, suggesting that rod-type morphology is advantageous for electron transport. The capacitance was also higher for the PEDOT-RTOMC than for the PEDOT-NTOMC, which is thought to be proportional to the surface area of the composite determined by the external and internal structure of the material.

Keywords: Conducting Polymer, PEDOT, Ordered Mesoporous Carbon, Vapor Phase Polymerization, Electrical Property

INTRODUCTION

Carbon materials, such as activated carbon, carbon black, nanotubes, and graphene, have great mechanical stability and large surface area which make them applicable to various functions such as fillers of a polymer composite [1-3], adsorbents for removing harmful substances [4,5], and catalyst supports [6,7]. In addition, they are also widely used as an electrode material for fuel cells [8], secondary batteries [9], and supercapacitors [10] due to excellent electrical conductivity. On the other hand, a family of mesoporous silica, named M41S such as MCM-41 and MCM-48, was developed by Mobil's research team in 1992 [11]. These mesoporous materials containing pores with diameters in the range 2-50 nm have been developed into different structures such as the SBA [12], MSU [13, 14] and KIT [15] series. A new dimension of carbon material, the ordered mesoporous carbon (OMC) having regular pores, has also been created utilizing the mesoporous silica previously mentioned as a template [16-18]. OMC offers the advantage of a regular pore structure with large surface area, with the pore size being easy to control. The morphological properties of SBA-15, which is a regular hexagonal array of one-dimensional nanopores, can control the morphology of the OMC [19]. SBA-15 template with controlled morphology had been used for the normal type ordered mesoporous carbon (NTOMC) [20] and the rod type ordered mesoporous carbon (RTOMC) [21-23], which are manipulated morphologies at the micro-sized level. Recently, the RTOMC has been reported to have a high specific capacitance and retention ratio, which makes it a potential material for next generation super capacitors [23].

Conductive polymers such as poly (3, 4-ethylenedioxythiophene) (PEDOT), polypyrrole (PPy) and polyaniline have been continuously studied since the discovery of polyacetylene [24]. Research on the combination of the conductive polymer and OMC materials has been conducted in an effort to improve the performances of these materials in the field of energy [25-27]. It has been previously reported that there is a 75% increase in the output density when the PEDOT-OMC composite is used as the anode material for supporting the Pt metal of the proton exchange fuel cell [25,26]. The discharge capacity and stability can also be improved with the use of PPy-OMC composite as a cathode material in a lithium-sulfur secondary battery [27]. The hybridization of the conductive polymer with the organic-inorganic material can be made in a variety of ways by the wet method [28,29]. Recently, we introduced organic-inorganic hybrid materials using vapor phase polymerization [30-35]. Vapor phase polymerization (VPP) can homogeneously produce multifunctional organic-inorganic composites at the molecular level, which cannot be achieved by simple solution-solution or solid-solution mixing. Also, polymerization carried out in the vapor

†To whom correspondence should be addressed.
E-mail: jhyim@kongju.ac.kr

phase allows the uniform coating of substances with complex shapes because the monomer in the gaseous phase can easily approach the interface of the solid [34-38].

In this study, we fabricated a hybrid composite by forming a conductive polymer layer *via* VPP on two types of OMCs of similar mesopores and sizes but different particulate morphologies. NTOMC and RTOMC underwent PEDOT VPP process to produce the hybrid composites. The morphological, chemical composition and pore structure of OMC and PEDOT-OMC composites were compared and analyzed. The electrical characteristics such as threshold voltage, electrical resistance, and capacitance of PEDOT-OMC composites were also compared.

MATERIALS AND METHODS

1. Chemicals

3,4-Ethylenedioxythiophene (EDOT, MD Bros.) as a monomer for PEDOT, iron (III) *p*-toluenesulfonate (FTS, ALDRICH) as oxidant and dopant and 1-butanol (JUNSEI, Japan) and ethanol (ALDRICH) as solvents were used without further purification. Two types of regular pore mesoporous carbon (OMC normal type: NTOMC, rod type OMC: RTOMC) were donated by UNICAM. NTOMC and RTOMC were synthesized by the methods described in the literature [20,21].

2. Preparation of PEDOT-OMC Composite

The PEDOT-OMC hybrid composites were prepared *via* VPP. FTS was added as an oxidizing agent to 1-butanol at 10, 15 and 20 wt% and was completely dissolved by stirring. The OMC was immersed in each FTS solution for 30 min and ultrasonicated in an ultrasonic washing machine (Power Sonic 410, Foshin Tech) to sufficiently allow the FTS to penetrate into the mesopores of the OMC. After filtering, FTS impregnated OMC was separated without any washing process and was dried in an oven at 60 °C for 10 min before it was transferred to a mesh pocket in the vapor phase polymerization reactor. Prior to the polymerization, nitrogen was allowed to flow into the reactor for 10 mL/s for 30 min to suppress the recrystallization of FTS. The VPP reactor used was the same as that reported in our literature [39]. EDOT, the monomer of PEDOT, was placed in a petri dish at the bottom of the reactor. The polymerization was carried out for 30 min at a maintained internal temperature of the reactor at 60 °C. The composite produced after polymerization was then immersed in ethanol for at least 1 h and washed with ethanol using a filtration apparatus. After washing, it was dried in an oven at 60 °C to obtain the final PEDOT-NTOMC and PEDOT-RTOMC hybrid composites.

3. Characterization of PEDOT-OMC Composite

Scanning electron microscopy (SEM, TESCAN, VEGA3, Czech) was used for particle surface and morphology analysis. The chemical composition and chemical species distribution of the PEDOT-OMC composite were analyzed by point and mapping analysis of energy dispersive X-ray spectroscopy (EDS, BRUKER, X FLASH, U.S.A.). Brunauer-Emmett-Teller (BET, Micromeritics ASAP 2020) analysis was performed to analyze the pore structure of OMC and PEDOT-OMC composites. The physically adsorbed moisture was completely removed by degassing the sample at 350 °C for 3 h prior to the analysis. At −196 °C, a nitrogen adsorption-desorption isotherm was obtained. The specific surface area was determined using the BET equation and the pore volume by the t-plot method. To measure the electrical properties of the PEDOT-OMC composites, the pellet was first formed into a disk with a diameter of 7 mm and a thickness of 0.5 mm. A silver line pattern with a thickness of 200-250 nm was deposited on a glass substrate using a thermal evaporator and the device was fabricated by connecting the deposited silver line and the prepared PEDOT-OMC composite disk using silver paste (Fig. 4(a)). The threshold voltage for turning on the light emitting diode (LED) was determined by connecting the fabricated device to a DC power supply (EXSO® K6133A, Korea) and gradually increasing the voltage. An inductor/capacitor/resistor (LCR) meter (GW INSTEK, LCR-6100, Taiwan) was used to measure the specific capacitance and resistance in parallel mode.

RESULTS AND DISCUSSION

1. Physico-chemical Structure Analysis of PEDOT-OMC Hybrid Composite

OMCs with various morphological characteristics have been reported using SBA-15 as a template for the OMC. Recently, a fiber type and a rod type OMC having the morphology of a one dimensional structure were applied to an electrode material of a supercapacitor. The specific capacitance was 162 F/g at a scan rate of 2 mV/s

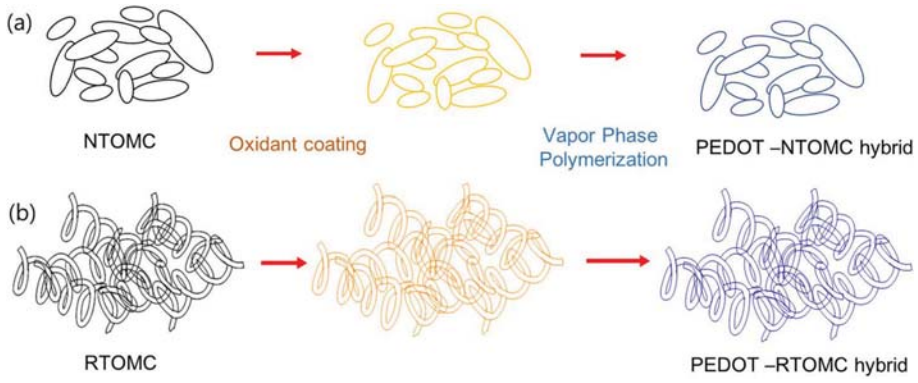

Scheme 1. Systematic preparation scheme of PEDOT coated mesoporous carbon: (a) Normal type mesoporous carbon (b) rod type mesoporous carbon.

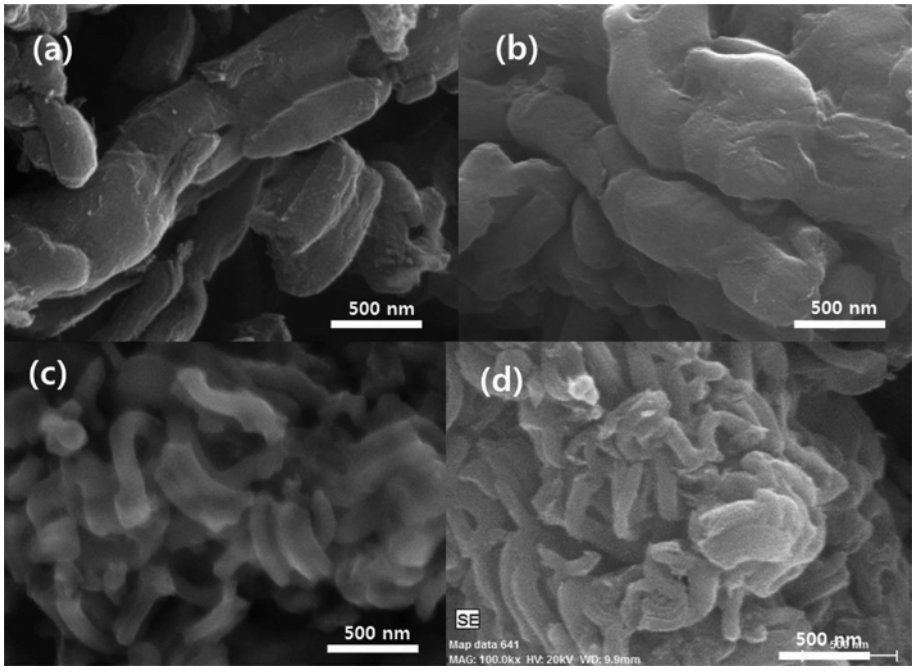

Fig. 1. SEM images of two kinds of mesoporous carbon: (a) NTOMC, (b) RTOMC and PEDOT coated mesoporous carbon (c) PEDOT-NTOMC hybrid, (d) PEDOT-NTOMC hybrid.

and 82% at 50 mV/s with RTOMC as an electrode material. These values are superior to that of the fiber type [23]. Previous studies also reported that improvement in the performance of the electrode as a fuel cell or secondary battery can be achieved by coating the OMC material with conductive polymer [26,27]. In our study, PEDOT-OMC composites were prepared by hybridizing OMC of two different morphologies with PEDOT *via* VPP (dry process) as shown in Scheme 1. The FTS solution is impregnated into the NTOMC or RTOMC and was made to enter the mesopores as well as the outer surface of the OMC. Uniform coating on the inner and outer surfaces of the mesoporous carbon could be possible when the EDOT VPP is applied to the mesoporous carbon impregnated with FTS. SEM images of NTOMC and RTOMC (Fig. 1(a), (c)) show that NTOMC has the shape of irregular elliptical particles of different sizes, and RTOMC shows the morphology of a twisted rod with a diameter of about 100-120 nm and a length of a few micrometers. Even after the two mesoporous carbons were hybridized with PEDOT, the surface morphology was maintained (Fig. 1(b), (d)), indicating that the conductive polymer layer was uniformly thinly coated. EDS analysis performed to analyze the chemical composition of PEDOT-OMC hybrid composites confirmed the presence of carbon alone on the NTOMC and

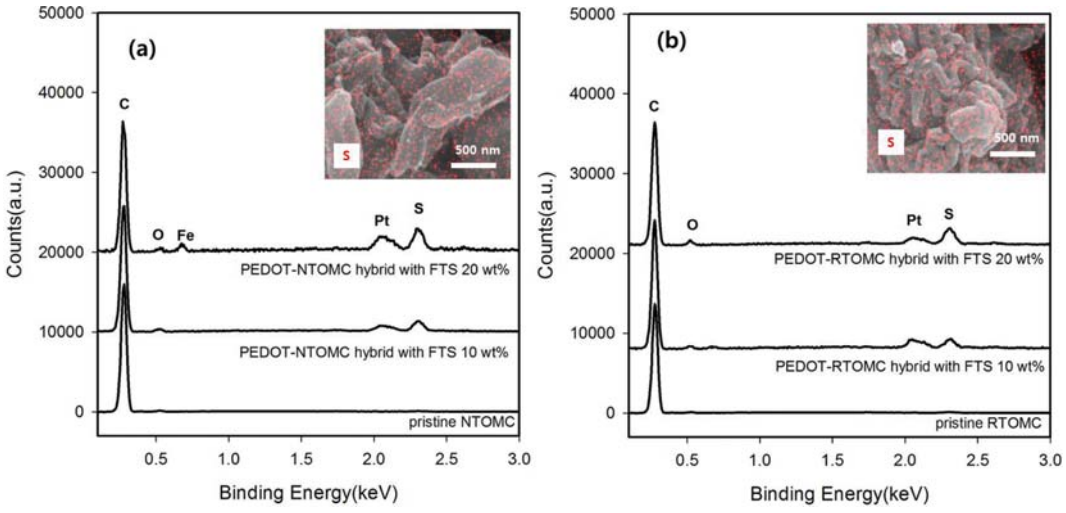

Fig. 2. EDS spectra of various mesoporous carbon of (a) NTOMC and PEDOT-NTOMC hybrid and (b) RTOMC and PEDOT-RTOMC hybrid as a function of FTS content.

Table 1. The content of sulfur in the PEDOT- ordered mesoporous carbon hybrid material as a function of FTS content

FTS contemt (wt%)	PEDOT-NTOMC hybrid		PEDOT-RTOMC hybrid	
	Atomic content (%)	Weight content (%)	Atomic content (%)	Weight content (%)
10	0.64	1.60	0.76	1.92
20	1.10	2.77	1.27	3.16

RTOMC mesoporous carbons with the peak at 0.27 eV as shown in Fig. 2. On the other hand, the peaks of oxygen (0.52 eV) and sulfur (2.30 eV) present in PEDOT were increased with increasing FTS content, indicating that the PEDOT layer was effectively polymerized on the OMC. Inset images of Fig. 2(a) and (b), showing the results of EDS mapping of sulfur atoms in the PEDOT-OMC composite subjected to VPP after 20 wt% FTS impregnation, show uniform distribution of the atoms, suggesting the uniform coating of PEDOT on the surface of the OMC. The quantitative content of sulfur atoms in the composite, on the other hand, is summarized in Table 1. The impregnation of OMC with 20 wt% of FTS resulted in the formation of about 3 wt% sulfur in the composite.

Table 2 summarizes the pore structure parameters, including the porosity, BET surface area and pore size of the two OMCs and the two PEDOT-OMC composites prepared therefrom. The pore sizes of pure NTOMC and RTOMC were 3.8 and 3.3 nm, respectively, and the BET surface area was 833 and 882 m^2/g. The porosity, BET surface area and pore size of the PEDOT-NTOMC and PEDOT-RTOMC composites decreased after VPP, and the reason for this reduction is thought to be the blockage of some parts of the mesopores after coating by PEDOT. The quantitative measure of the reduction of the pore size is 0.2-0.4 nm. Fig. 3 shows the N_2 adsorption-desorption isotherms and pore size distribution curves of NTOMC, PEDOT-NTOMC, RTOMC and PEDOT-RTOMC. All samples exhibit type IV hysteresis specified by the IUPAC classification, thus indicating that the mesopores are present. Despite the decrease in adsorbed nitrogen, similar shape of hysteresis loops is

Table 2. Summary of nitrogen BET analysis for two kinds mesoporous carbon and PEDOT coated ordered mesoporous materials

Sample	Pore volume (cm^3g^{-1})	[a]S_{BET} (m^2g^{-1})	Pore size (nm)
NTOMC	0.93	833	3.8
PEDOT-NTOMC hybrid [b]	0.57	507	3.4
RTOMC	0.94	882	3.3
PEDOT-RTOMC hybrid [b]	0.59	546	3.1

[a]BET surface area

[b]Hybrid samples prepared by VPP with 20 wt% FTS

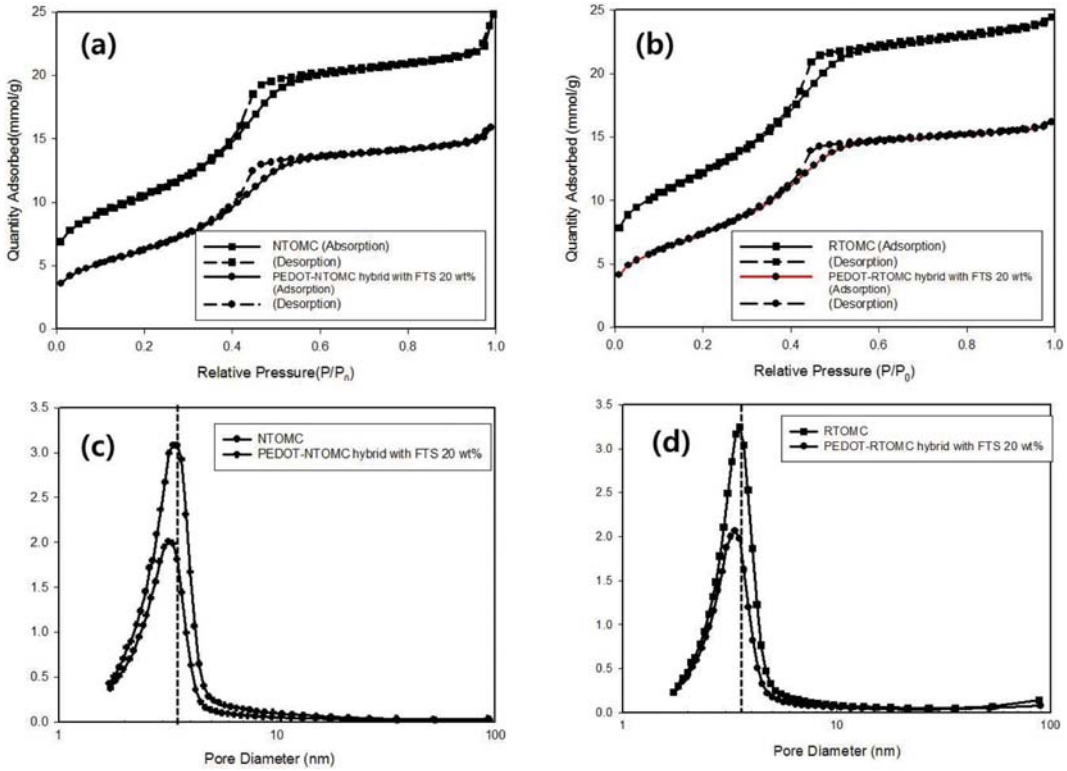

Fig. 3. Nitrogen adsorption-desorption isotherms and pore size distribution of PEDOT-mesoporous carbon hybrid material prepared with 20 wt% FTS (a), (c) PEDOT-NTOMC hybrid, (b), (d) PEDOT-RTOMC hybrid.

observed for both the adsorption isotherms of NTOMC and RTOMC and the PEDOT-OMC hybridized by VPP process. This means that there was no change in the pore shape of the original OMC. The pore size of each carbon material, on the other hand, decreased slightly after the conductive polymer layer PEDOT was coated on the walls of the mesopores (see Table 2). However, the shape of all characteristic pore size distribution curves of all PEDOT-OMC hybrid composites did not change as shown in Fig. 3(c) and (d).

2. Electrical Characteristics of PEDOT-OMC Hybrid Composite

A simple device for measuring the electrical properties of PEDOT-OMC hybrid composites was fabricated as shown in Fig. 4(a). A DC power supply was connected to the device to measure the threshold voltage in turning on a light emitting diode (LED). The threshold voltage of PEDOT-NTOMC and PEDOT-RTOMC was 1.4 V. In the case of PEDOT-NTOMC, a voltage of 1.5 V was applied

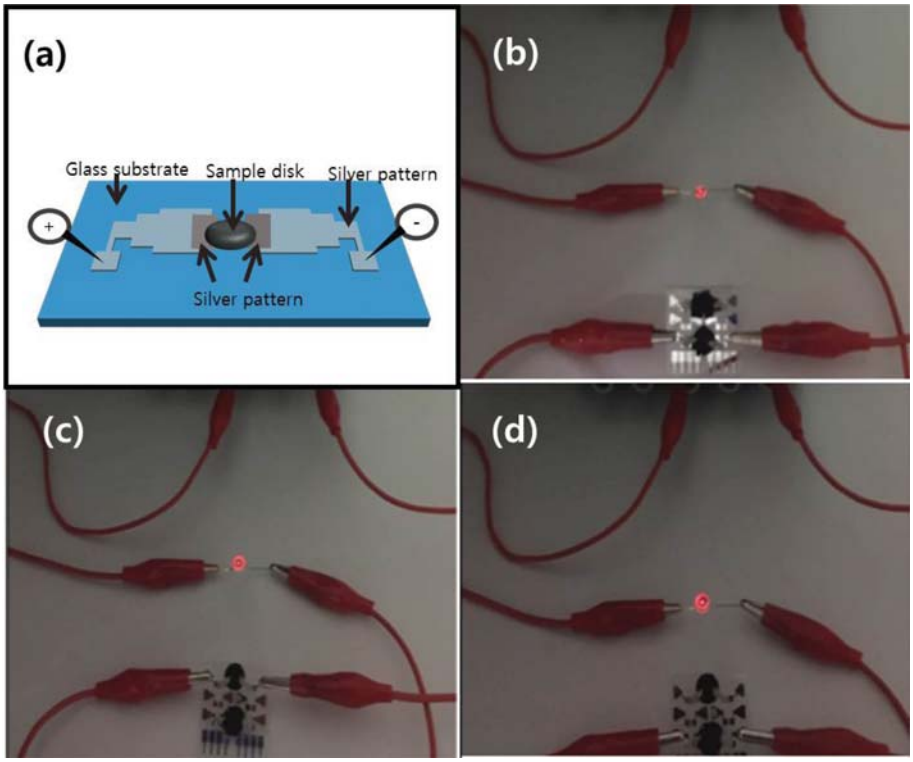

Fig. 4. Brightness comparison of LED bulb in PEDOT-NTOMC hybrid as a function of FTS content: (a) Test device (b) PEDOT-NTOMC with FTS 10 wt%, (c) PEDOT-NTOMC with FTS 15 wt%, (d) PEDOT-NTOMC with FTS 20 wt%, applied voltage was fixed at 1.5 V.

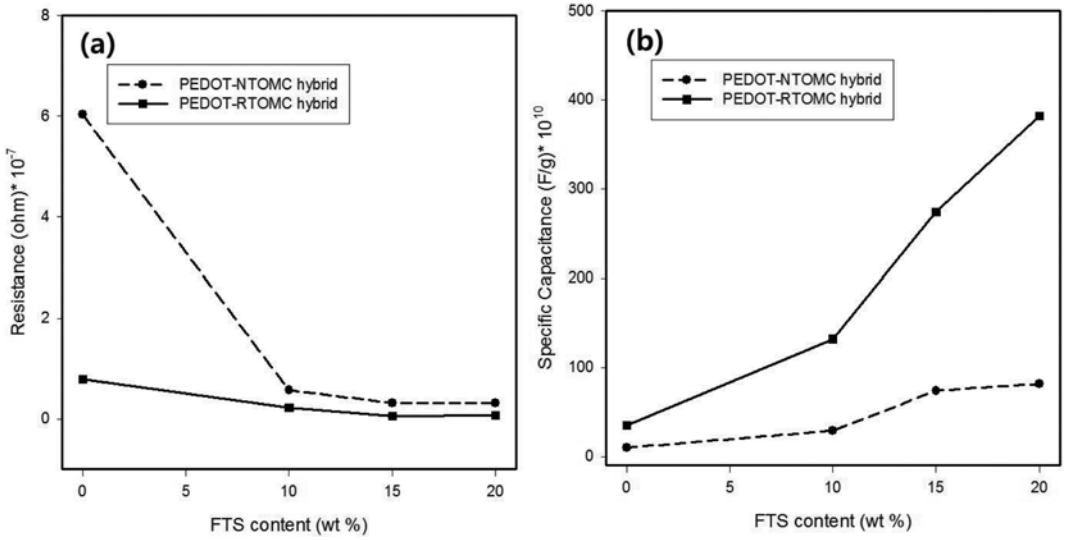

Fig. 5. Comparisons of electrical properties of two kinds of PEDOT- mesoporous carbon hybrid: (a) Resistance and (b) specific capacitance behavior as functions of FTS content.

to the fabricated device equipped with the samples and an increase in the brightness of the LED bulb was observed with an increase in the content of FTS in the composite material. This might be due to the decrease in the electrical resistance of the test disc as the conductive PEDOT layer becomes thicker with increasing FTS content. Quantitative electrical properties were determined by LCR meter and the results are illustrated in Fig. 5 where the capacitance and electrical resistance of PEDOT-OMC is plotted as a function of the FTS content. The resistance decreased with an increase in the FTS concentration as shown in Fig. 5(a). The PEDOT-RTOMC exhibited lower resistance than PEDOT-NTOMC at all concentrations of FTS. It might be because the transport path of electrons in the RTOMC composite, which shows morphological characteristics of the rod shape, is much more developed than the NTOMC system. Also, the capacitance tended to increase as a function of the FTS content (Fig. 5(b)). Moreover, the capacitance of PEDOT-RTOMC was larger than that of PEDOT-NTOMC for the same FTS concentration. The capacitance difference of the two composites also tended to increase as the FTS content increased. This phenomenon may be related to the surface area of the mesoporous composites determined by the external and internal structure of the material. In general, the capacitance of a material is proportional to the dielectric constant and the contact area, and is inversely proportional to the distance between the electrodes. The tests were performed under the assumption that the OMC-based composites prepared were made of disks of the same size, so that the electrode distance and the dielectric constant were also similar. The surface area of PEDOT-RTOMC is larger than that of PEDOT-NTOMC as shown in Table 2. Therefore, the capacitance may be proportional to the surface area of the mesoporous carbon system.

CONCLUSIONS

A hybrid conductive composite with PEDOT layer formed by VPP in two types of OMC (NTOMC, RTOMC) with different morphologies was successfully fabricated. The PEDOT layer was observed to uniformly coat the OMC, thereby not changing the surface morphology of the original mesoporous carbon material. The amount of PEDOT in the composite increased as the amount of FTS, the oxidant used in VPP, was increased. Pore s ize, porosity, and surface area decreased as the PEDOT was coated on the outer surface of the OMC and the mesopore inner wall. The electrical resistance of the PEDOT-RTOMC composite was lower than that of the PEDOT-NTOMC composite because the rod-shaped morphology is advantageous for electron transport. In the case of the capacitance, the PEDOT-RTOMC composite was higher than the PEDOT-NTOMC composite, which is probably due to the difference in surface area of t he PEDOT-OMC composite. The VPP-based PEDOT-OMC hybrid composites provided in this study can therefore be effectively used as electrode materials for fuel cells, secondary batteries, and capacitors.

ACKNOWLEDGEMENTS

This work was supported by the research grant of the Kongju National University in 2018.

REFERENCES

1. K. Wakabayashi, C. Pierre, D. A. Dikin, R. S. Ruoff, T. Ramanathan, L. C. Brinson and J. M. Torkelson, *Macromolecules*, **41**(6), 1905 (2008).
2. I. Balberg, *Carbon*, **40**(2), 139 (2002).
3. T. Kuilla, S. Bhadra, D. Yao, N. H. Kim, S. Bose and J. H. Lee, *Prog. Polym. Sci.*, **35**(11), 1350 (2010).
4. S. N. Hussain, E. P. L. Roberts, H. M. A. Asghar, A. K. Campen and N. W. Brown, *Electrochim. Acta*, **92**(1), 20 (2013).
5. J. L. Gong, B. Wang, G.-M. Zeng, C.-P. Yang, C.-G. Niu, Q.-Y. Niu, W.-J. Zhou and Y. Liang, *J. Hazard. Mater.*, **164**(2-3), 1517 (2009).
6. Y. Liang, H.-B. Dai, L.-P. Ma, P. Wang and H.-M. Cheng, *Int. J. Hydrogen Energy*, **35**(7), 3023 (2010).
7. Y.-F. Li, M.-Q. Guo, S.-F. Yin, L. Chen, Y.-B. Zhou, R.-H. Qiu and C.-T. Au, *Carbon*, **55**, 269 (2013).
8. C. A. Bessel, K. Laubernds, N. M. Rodriguez and R. T. K. Baker, *J. Phys. Chem. B*, **105**(6), 1115 (2001).
9. M. Nie, D. Chalasani, D. P. Abraham, Y. Chen, A. Bose and B. L. Luch, *J. Phys. Chem. C*, **117**(3), 1257 (2013).
10. J. Ji, L. L. Zhang, H. Ji, Y. Li, X. Zhao, X. Bai, X. Fan, F. Zhang and R. S. Ruoff, *ACS Nano*, **7**(7), 6237 (2013).
11. C. T. Kresge, M. E. Leonowicz, W. J. Roth, J. C. Vartuli and J. S. Beck, *Nature*, **359**, 710 (1992).
12. D. Zhao, J. Feng, Q. Huo, N. Melosh, G. H. Fredrickson, B. F. Chmelka and G. D. Stucky, *Science*, **279**(5350), 548 (1998).
13. P. T. Tanev and T. J. Pinnavaia, *Science*, **267**, 865 (1995).
14. Y. Liu, W. Zhang and T. J. Pinnavaia, *Angew. Chem. Int. Ed.*, **40**(7), 1255 (2001).
15. R. Ryoo, J. M. Kim, C. H. Ko and C. H. Shin, *J. Phys. Chem.*, **100**, 17718 (1996).
16. S. H. Joo, S. J. Choi, I. Oh, J. Kwak, Z. Liu, O. Terasaki and R. Ryoo, *Nature*, **412**, 169 (2001).
17. J. Lee, K. Sohn and T. Hyeon, *J. Am. Chem. Soc.*, **123**, 5146 (2001).
18. J. Lee, J. Kim and T. Hyeon, *Adv. Mater.*, **18**, 2073 (2006).
19. H. I. Lee, J. H. Kim, G. D. Stucky, Y. Shi, C. Pak and J. M. Kim, *J. Mater. Chem.*, **20**, 8483 (2010).
20. H. I. Lee, J. H. Kim, D. J. You, J. E. Lee, J. M. Kim, W.-S. Ahn, C. Pak, S. H. Joo, H. Chang and D. Seung, *Adv. Mater.*, **20**, 757 (2008).
21. C. Chae, J. H. Kim, J. M. Kim, Y.-K. Sun and J. K. Lee, *J. Mater. Chem.*, **22**, 17870 (2012).
22. C. Yu, J. Fan, B. Tian, D. Zhao and G. D. Stucky, *Adv. Mater.*, **14**, 1742 (2002).
23. Y. Xiao, H. Dong, B. Lei, H. Qiu, Y. Liu and M. Zheng, *Mater. Lett.*, **138**, 37 (2015).
24. C. K. Ching, C. R. Fincher, Y. W. Park, A. J. Heeger, H. Shirakawa, E. J. Louis, S. C. Gau and A. G. MacDiarmid, *Phys. Rev. Lett.*, **39**, 1098 (1977).
25. J. Wang, X. Yu, Y. Li and Q. Liu, *J. Phys. Chem. C*, **111**(49), 18073 (2007).
26. K. K. Tintula, A. K. Sahu, A. Shahid, S. Pitchumani, P. Sridhar and A. K. Shukla, *J. Electrochem. Soc.*, **157**(11), B1679 (2010).
27. G. Ma, Z. Wen, J. Jin, Y. Lu, K. Rui, X. Wu, M. Wu and J. Zhang, *J. Power Sources*, **254**, 353 (2014).
28. Y. Wei, J.-M. Yeh, D. Jin, X. Jia, J. Wang, G.-W. Jang, C. Chen and R. W. Gumbs, *Chem. Mater.*, **7**, 969 (1995).

29. A. G. Sommers,*World Patent*, WO 99/58464 (1998).
30. Y.-H. Han, J. Travas-Sejdic, B. Wright and J.-H. Yim, *Macromol. Chem. Phys.*, **212**, 521 (2011).
31. J.-H. Yim, *Compos. Sci. Technol.*, **86**, 45 (2013).
32. R. Khadka and J.-H. Yim, *Macromol. Res.*, **23**, 559 (2015).
33. Y. S. Ko and J.-H. Yim, *Polymer*, **93**, 167 (2016).
34. S. W. Kim, S. W. Lee, J. Kim, J.-H. Yim and K. Y. Cho, *Polymer*, **102**, 127 (2016).
35. J. S. Choi, J. S. Park, B. Kim, B.-T. Lee and J.-H. Yim, *Polymer*, **120**, 95 (2017).
36. J. Lock, S. Im and K. Gleason, *Macromolecules*, **39**, 5326 (2006).
37. S. G. Im and K. K. Gleason, *Macromolecules*, **40**, 6552 (2007).
38. A. Asatekin, M. C. Barr, S. H. Baxamura, K. K. S. Lau, W. Tenhaeff, J. Xu and K. K. Gleason, *Mater. Today*, **13**(5), 26 (2010).
39. J. Ahn, S. Yoon, S. G. Jung, J.-H. Yim and K. Y. Cho, *J. Mater. Chem. A.*, **5**, 21214 (2017).